

Mechanochemical synthesis of nanostructured BiVO₄ and investigations of related features

R. Venkatesan^{a,c}, S. Velumani^{a,b,**}, A. Kassiba^{c,*}

^a Nanoscience and Nanotechnology program, CINVESTAV-IPN, Zacatenco, Av IPN #2508, Col Zacatenco, D.F., C.P. 07360, Mexico

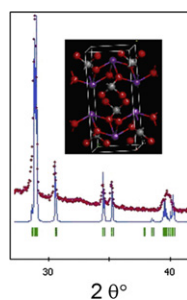
^b Department of Electrical Engineering (SEES), CINVESTAV-IPN, Zacatenco, Av IPN #2508, Col Zacatenco, D.F., C.P. 07360, Mexico

^c Institute of Molecules & Materials of Le Mans (IMMM) UMR CNRS, Universite du Maine, 72085 Le Mans, France

HIGHLIGHTS

- ▶ Synthesis by ball-milling of original nanostructures of BiVO₄.
- ▶ Stabilizing a monoclinic BiVO₄ polype with nanoparticle sizes about 20 nm.
- ▶ Investigations of annealing effects on structures, vibration and optical features.

GRAPHICAL ABSTRACT



ARTICLE INFO

Article history:

Received 27 December 2011

Received in revised form

27 April 2012

Accepted 25 May 2012

Keywords:

BiVO₄

Ball milling

XRD

Raman

Nanoparticles

ABSTRACT

Highly crystalline monoclinic bismuth vanadate (BiVO₄) nanopowders with crystallite sizes less than 50 nm were obtained by mechanical milling of a stoichiometric mixture of bismuth oxide (Bi₂O₃) and vanadium pentoxide (V₂O₅). Different synthesized batches were obtained by varying the preparation times and the number of the tungsten carbide balls (BPR) while keeping constant the jar rotation speed. Annealing treatments were performed on the obtained nanopowders in order to improve the crystalline order and the BiVO₄ nanoparticles surface states. Characterizations methods, X-ray diffraction (XRD), field emission scanning electron microscopy (FESEM) equipped with X-ray energy dispersive spectrometer (EDS), Raman spectrometry, FTIR and UV–Vis diffuse reflectance techniques were used to shed light on the structure, morphologies and composition of the obtained nanopowders. Even if monoclinic BiVO₄ crystalline structure was stabilized in samples after appropriate annealing, shifts of Raman peak positions after such treatments revealed the occurrence of symmetry distortions in the local structure of the monoclinic phase.

© 2012 Elsevier B.V. All rights reserved.

1. Introduction

Semiconducting composites with hetero-junction structures are of great interest for photocatalytic (PC) and photovoltaic (PV)

applications [1]. This includes PC processes leading to hydrogen based clean energy, degradation of organic pollutants or waste water treatments [2]. In this context, TiO₂ is the most experienced even if its band gap in the range 3.2 eV limits the efficiency with regard to the absorption of the only UV radiation of the solar spectrum [3]. In order to make PC activity more effective, an increase of the absorbed spectral range is required. This is achieved notably by doping the material by suitable elements which will be able to induce intermediate levels in the band gap [4]. An alternative approach can be also searched through the use of photoactive titanium oxide based gels [5]. However, the search for

* Corresponding author. Tel.: +33 243833512.

** Corresponding author. Nanoscience and Nanotechnology program, CINVESTAV-IPN, Zacatenco, Av IPN #2508, Col Zacatenco, D.F., C.P. 07360, Mexico. Tel.: +52 55 5747 4001.

E-mail addresses: velu@cinvestav.mx (S. Velumani), kassiba@univ-lemans.fr (A. Kassiba).

intrinsically active and stable materials represent challenging tasks and this is the motivation of our present work to offer an alternative PC active materials based on nanostructured bismuth.

Among the considered structures, bismuth vanadate represents promising option as one of the non-titania based visible light driven semiconductor photocatalyst. BiVO_4 was first suggested by Kudo et al. [6] for water dissociation, due to its narrow band gap. Beyond the thought innovative PC applications, this material was basically used as high performance pigments compared to organic based paintings. It is also classified as environment friendly and could replace toxic pigments such as cadmium or lead-based paints.

From structural aspects, BiVO_4 exist in three forms with the features of tetragonal zircon, monoclinic and tetragonal scheelite [7]. The performance of the semiconducting photocatalyst is intimately dependant on the morphology, crystalline phase, preparation method and surface area of the catalyst. Compared to the tetragonal BiVO_4 with a band gap about 2.9 eV and then mainly absorbing in the UV range, the monoclinic polytype with 2.4 eV as band gap, exhibits higher photocatalytic performance [6].

Several bismuth based oxides have been successfully prepared by different techniques such as co-precipitation [8,9], solution combustion method [10], microwave irradiation [11], mild hydrothermal [12,13], sonochemical method [14], metal organic decomposition [15], ultrasonic spray pyrolysis [2] and solid state reaction [16]. The last process exemplified by ball milling, is particularly relevant to obtain nanostructured materials with large specific area as reported below.

Thus, the present work is dedicated to mechanochemical synthesis of BiVO_4 by high energy ball milling process and optimization of parameters like milling times as well as the ball to powder ratio (BPR) and annealing temperatures. The objective of the work is to reduce the milling time in order to obtain nanostructured materials with single crystalline phase and improved crystalline order and nanoparticle surface states. Following the synthesis, the investigations of the structural, vibrational and optical properties were carried out and theoretical simulations were performed to verify the involved structures. Even though synthesis conditions were varied in a large extent, the present report is limited to samples obtained by 6 h and 11 h as milling times with various BPR. In addition, annealing at 450 °C was performed in order to improve the crystalline order and the surface states of nanoparticles. With such parameters, relevant structural and optical features were obtained and open possibilities for promising applications in photocatalysis.

2. Experimental detail

2.1. Synthesis

BiVO_4 samples were prepared by the milling of pure bismuth oxide (99.999%, Sigma–Aldrich) and vanadium oxide (99.99%, Sigma–Aldrich) using a Retsch-planetary ball mill PM 400. All chemicals were analytical grade and used without further purification. Mixtures about 8 g were homogenized by suitable grinding using agate mortar and put into an 80 ml tungsten carbide jar with tungsten carbide balls of 10 mm diameter.

It is generally recognized that three stages take place in a mixed oxide powder during high-energy ball milling process. It involves (i) refinement of crystallites (ii) nucleation of a new phase from highly reactive powders activated by high energy ball milling, and (iii) crystallization and crystal growth of the newly-formed phase [17]. During the initial ball milling, the powders were mixed homogeneously and the strong mechanical collision between the

two powder particles might induce their metallurgical chemical contacts [18].

The sample was mechano-chemically activated in air atmosphere using different balls to powder weight ratio BPR (5:1, 8:1 and 10:1) with 6 h and 11 h as a milling time. Selected powders were annealed at 450 °C under air for 1 h. The samples hereafter will be designated with a rule illustrated as the example “11 h8:1” which means, powders milled for 11 h with a ball to powder ratio of 8:1 and for annealed it is represented as 11 hA8:1.

2.2. Characterization methods

The crystalline structures of the different BiVO_4 batches were investigated by X-ray diffraction (XRD) using the $\text{CuK}\alpha$ radiation ($\lambda = 1.5406 \text{ \AA}$). The primary particle size, shape and morphology were investigated by field emission scanning electron microscope (FESEM). Powder samples were dispersed ultrasonically in water and a few drops of the dispersion were dried directly on carbon for FESEM analysis respectively. The FESEM analysis was performed by Carl Zeiss Auriga 60, nanotechnology system.

Raman spectra were recorded in the same conditions for all the examined samples by a Horiba Jobin Yvon, with a 632.8 nm He–Ne laser source used as excitation line. The diffuse reflectance spectra were measured with a Cary 500 UV–VIS–NIR spectrophotometer working in the spectral range 200–1100 nm. The FT-IR spectra were recorded on pellets made from the concerned sample and with KBr mixture, by using Nicolet 510 spectrometer which allows to perform Fourier transform infrared spectroscopy (FTIR) in the wave number range 4000–400 cm^{-1} .

3. Result and discussion

3.1. X-ray diffraction and simulation studies

Fig. 1 (A–D) shows the XRD patterns of BiVO_4 powders obtained by ball milling for time durations 6 h and 11 h with different ball to powder weight ratios (BPR). At first glance, the reflections can be readily assigned to a pure monoclinic scheelite phase with the space group $I2/a$ with lattice constants $a = 0.5195 \text{ nm}$, $b = 1.1701 \text{ nm}$ and $c = 0.5092 \text{ nm}$ which is in agreement with the data card JSPDS number 00-014-0688 for the samples 6 h10:1, 11 h8:1, 11 h10:1, 6 hA10:1, 11 hA8:1 and 11 hA10:1. For the remaining samples it was observed BiVO_4 monoclinic phase along with the precursor Bi_2O_3 monoclinic phase, this might be due to the incomplete mechanochemical reaction because of the milling time along with number of balls used. Or this reveals the number of balls and the milling time used is not sufficient to complete the mechanochemical reaction to form pure form of BiVO_4 [1]. Based on simulations procedures, a quantitative analysis was carried out to identify the involved crystalline structures obtained by ball milling. Simulation studies were performed using the DFT approach as implemented in the commercial CASTEP code [19]. The ultrasoft pseudopotential was chosen in the calculations because of its advantages in both efficiency and credibility. Basic structure of BiVO_4 in the monoclinic phase is constructed by using crystallographic atomic positions and refined via DFT–LDA. Simulated structure of the monoclinic scheelite BiVO_4 is shown in Fig. 2 with the unit cell depicted in inset of Fig. 2 with a content of four bismuth, four vanadium atoms and sixteen oxygen atoms. Fig. 2 gives also a comparison between XRD patterns of simulated monoclinic scheelite BiVO_4 structure and the powder prepared by 6 h10:1 and annealed at 450 °C for 1 h. For this sample, additional reflections remain observed and attributed to Bi_2O_3 monoclinic phase. Increasing the milling time up to 11 h leads to pure

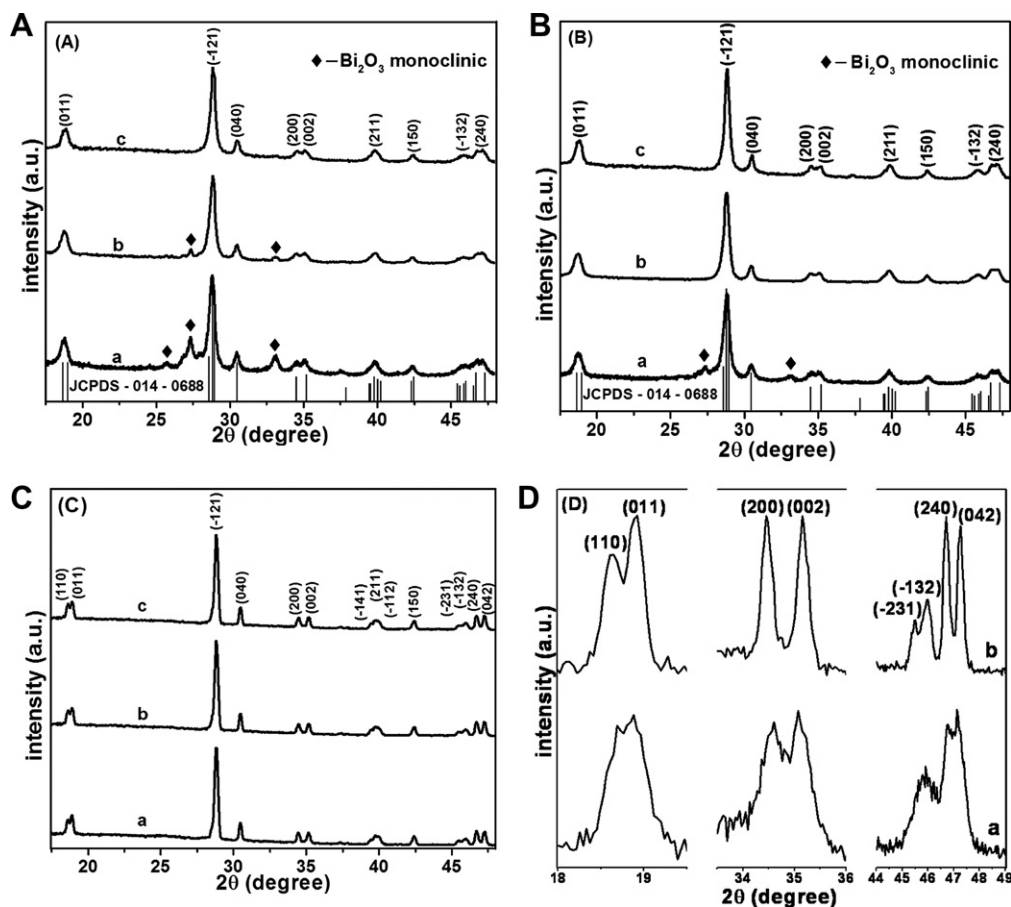


Fig. 1. XRD patterns of BiVO_4 samples prepared under different conditions. (A) Samples prepared under different BPR with 6 h milling time: a) 6 h5:1, b) 6 h8:1 and c) 6 h10:1. (B) Samples prepared under different BPR with 11 h milling time: a) 11 h5:1, b) 11 h8:1 and c) 11 h10:1. (C) Milled-annealed samples: a) 6 hA10:1, b) 11 hA10:1, c) 11 hA8:1. (D) The magnified XRD patterns near 18.5° , 35° and 47° : a) 6 h10:1 and b) 6 hA10:1.

monoclinic scheelite structure of BiVO_4 as also revealed by XRD diagram fitting by using FullProf software (Fig. 3).

From XRD patterns and the Scherrer law, average particle sizes were estimated roughly in the range 18–21.6 nm for 6 h and 11 h milling time and also by increasing number of used milling balls. The BPR parameter plays an important role in the complete transformation of BiVO_4 from the precursor's mixture, although the transformation could be achieved at 11 h8:1. Additionally to these effects, annealing plays a key role in the increase of nanoparticles

sizes. Indeed, as a result of annealing at 450°C the average particle size always increases and the particle size distribution widens. The average particle sizes were found in the order of 45 nm to few micrometers. Meanwhile, improved crystalline structures are also realized by annealing as exemplified through the well resolved splitting which manifests on the diffraction patterns (Fig. 1D). As indicated, the reflection (011) splits into (110) and (011), this is also the case for (200) and (002) being well separated as also observed for (240) and (042) reflections.

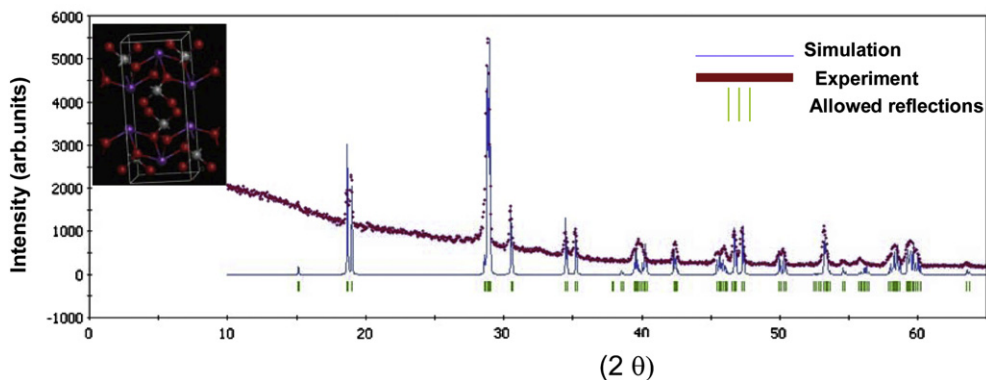


Fig. 2. Experimental and simulated XRD patterns of monoclinic scheelite BiVO_4 . The simulation is based on DFT calculations implemented in CASTEP software. The inset shows the characteristic unit cell of BiVO_4 .

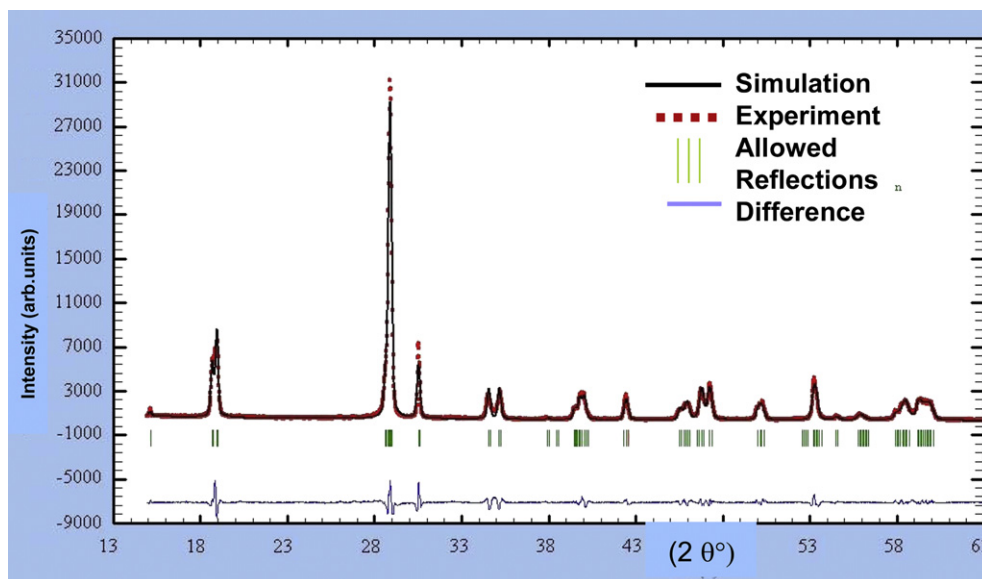


Fig. 3. XRD pattern the monoclinic BiVO_4 sample obtained by 11 h milling and annealed at 450°C during 1H: experimental (Yobs) and simulated (Ycal) by using FullProf software.

3.2. Surface morphology

3.2.1. Field emission scanning electron microscopy (FESEM)

FE-SEM microphotographs of the synthesized BiVO_4 nanopowders are shown in Fig. 4. The agglomerations observed in all micrographs result from electrostatic forces at the interfaces and also from Van der Waals interactions [20]. From visual examination of Fig. 4, the as-prepared samples are composed by small particles of spherical shape with the occurrence of agglomerations. The X-ray diffraction lines are used to evaluate the average size of coherent diffraction domains to be close to 20 nm. For the annealed samples, a net coalescence of the particles occurs leading to quite large particles with also an improved crystalline order. However, the agglomerations (\sim micrometer) give rise to different appearance of the samples, which can be induced by different reactive surfaces.

The different morphologies observed in the samples point out a major role played by milling time and BPR parameter. Annealing alters significantly the grain size and also the morphology of samples. Kinetic energy of the medium and possibility of occurrence of exothermic process contribute to local heating of powder during milling. Beyond to lead to the morphology changes, these processes improve the crystalline structures as also demonstrated by XRD investigations. It is worth to mention that as it was performed, the mechanochemically assisted synthesis contributes to realize BiVO_4 nanoparticle with sizes among the smallest compared to former reports [21,22].

3.3. Raman investigations

Raman spectrometry is a powerful tool to analyze the vibrational properties of materials in close relation with the organization of the involved structures. As illustrated in Fig. 5, Raman spectra of the as prepared BiVO_4 samples exhibits characteristic fingerprints with clear dependence on the duration of milling and on the BPR parameter. The main Raman bands located at 211, 327, 369, 710 and 828 cm^{-1} are consistent with typical vibrational bands of BiVO_4 structures [23,24]. The Raman features around 710 (weak signal) and 828 cm^{-1} (intense band) were attributed to the stretching modes of two different types of V–O bonds. Precisely, these

frequencies are consistent with asymmetric V–O stretching for 710 cm^{-1} while the 828 cm^{-1} correspond to V–O symmetric vibration mode. In the low wavenumber regions, the bands at 327 and 369 cm^{-1} are related to bending modes of the VO_4 tetrahedrons. The Raman band at 210 cm^{-1} also involved for monoclinic bismuth vanadates did not reflect any noticeable difference between different samples. In contrast, the bands at 327 and 369 cm^{-1} are quite sensitive to the synthesis conditions with regard to the different line widths, line splitting and line positions. This is also the case of stretching vibrational mode leading to the band at 832 cm^{-1} which traduces the changes on structural variations in the investigated samples. Particularly, milling and annealing contribute to shift the 832 cm^{-1} band to low frequencies in comparison with the band of only milled samples. Moreover, with the crystalline structure improvement by the thermal treatment, the full width half maximum of the intense Raman band decreases (inset in Fig. 3) as also does the vibration frequency of V–O bond. Such observation is consistent with stretching vibrational Raman bands being associated to longer bond lengths. This is well illustrated from the functional relationship between the Raman stretching frequencies and the metal–oxygen bond lengths in the involved crystalline structures [25–27].

To sum up, Raman spectra correlate the annealing effect and the induced improvement of the particle surface states and the crystalline structures for all considered samples. This treatment acts in more drastic way compared to the time duration or the mechanical milling conditions (BPR). Additionally, the main features of Raman spectra are consistent with the stabilized crystalline structure as a pure monoclinic phase in agreement with the structural data obtained by XRD investigations.

3.4. Optical properties

3.4.1. UV–diffuse reflectance spectroscopy (DRS)

The performed DRS experiments are dedicated to compare the optical behavior of the as prepared and annealed BiVO_4 powders as summarized in Fig. 6. All the curves show similar features and the same tendency of the changes with annealing. An extrapolation of the curves to the wavelength axis allows estimating band gaps, which is summarized and given in Table 1. The electronic structure

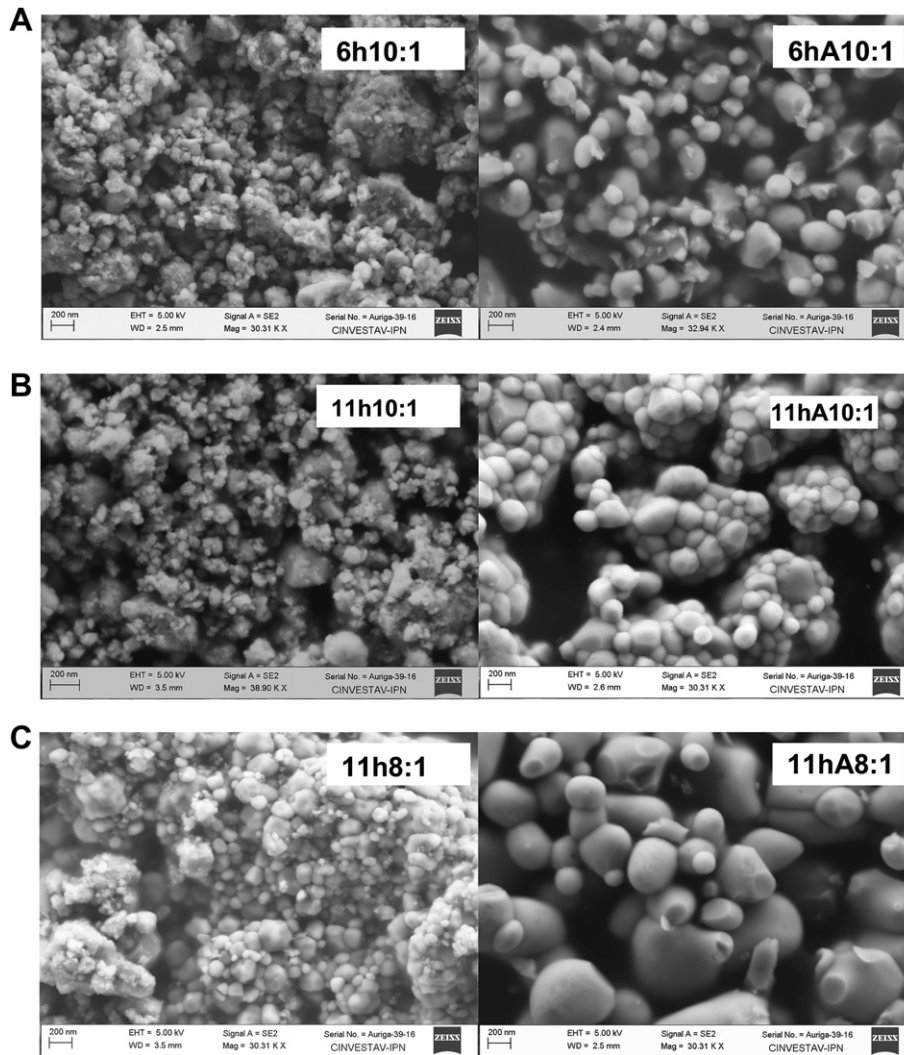


Fig. 4. FESEM images of the mechanochemically synthesized BiVO_4 nanoparticles. A) As prepared and annealed samples at 6 h with 10:1 BPR. B) As prepared and annealed samples at 11 h with 10:1 BPR. C) As prepared and annealed samples at 11 h with 8:1 BPR.

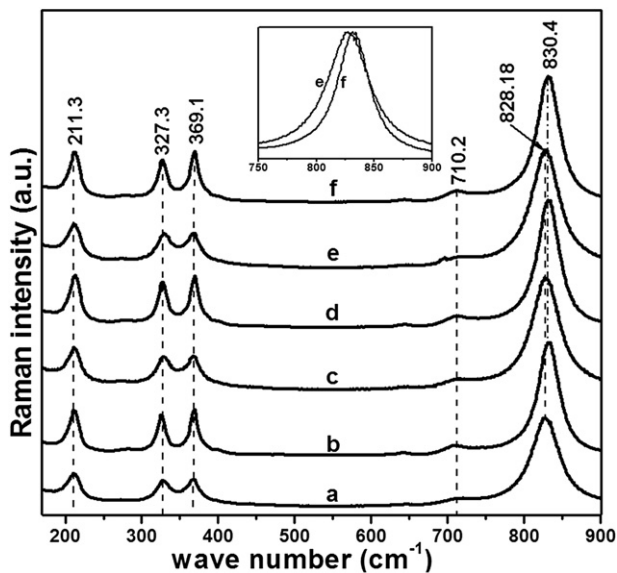


Fig. 5. Raman spectra of the ball milled samples in the defined conditions: a) 6 h10:1, b) 6 hA10:1, c) 11 h10:1, d) 11 hA10:1, e) 11 h8:1 and f) 11 hA8:1. Inset: frequency shift and FWHM decrease with annealing.

of BiVO_4 can be outlined briefly in order to account for the optical behavior. In this aim, it is worth noting that the valence band is formed by the hybrid orbitals of Bi 6s and O 2p while the conduction band results from unoccupied V 3d states. Even if the electronic band extrema are located outside the Brillouin zone center, BiVO_4 exhibits the features of direct band gap semiconductor, i.e. it maintains favorable low energy direct transitions [28]. The obtained values of the band gap are consistent with monoclinic BiVO_4 . Comparing with the milled and milled-annealed samples, absorption edge of the BiVO_4 powder was blue-shifted probably due to the aggregation of the BiVO_4 particles. The milled samples contain smaller particles in comparison with milled annealed ones. As a consequence, the blue shift of the band gap from 2.3 to 2.4 eV can be explained by some confinement effects when the involved nanocrystals can be smaller than the Bohr radius of excitons in such structures. However, it is well known that beyond to improve the crystalline features, the annealing modifies the particles surface states and suppress all active electronic centers which can result from dangling bonds or disorder at the outermost particle surfaces. The suppression of the surface electronic centers by annealing and the increase of particle sizes contribute to changes on the absorption spectra of the BiVO_4 samples.

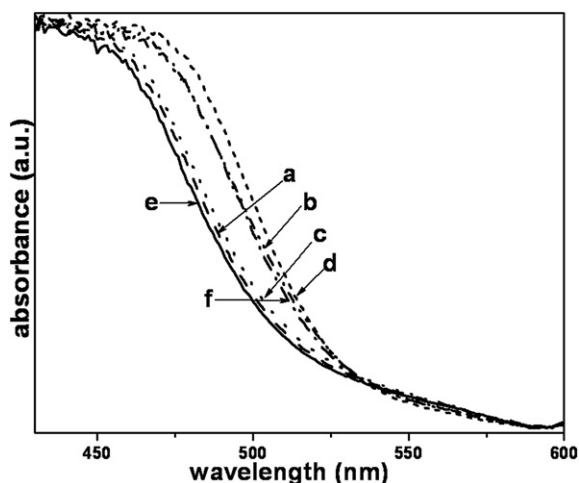


Fig. 6. UV–visible diffuse reflectance spectra of the as prepared samples: a) 6 h10:1, b) 6 hA10:1, c) 11 h10:1, d) 11 hA10:1, e) 11 h8:1 and f) 11 hA8:1.

Table 1

Band gap absorption edges determined from diffuse reflectance experiments performed on the BiVO_4 crystallites synthesized by ball milling with and without annealing.

Samples reference	Absorption edge (nm)	Band gap (eV)
6 h10:1	518	2.39
6 hA10:1	530	2.34
11 h10:1	520	2.38
11 hA10:1	532	2.33
11 h8:1	515	2.40
11 hA8:1	530	2.34

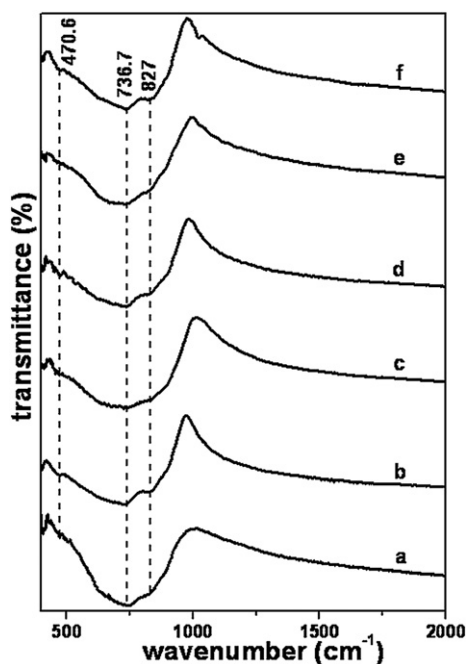


Fig. 7. FTIR spectra of BiVO_4 obtained under different time durations of milling and after annealing: a) 6 h10:1, b) 6 hA10:1, c) 11 h10:1, d) 11 hA10:1, e) 11 h8:1 and f) 11 hA8:1.

3.4.2. FT-IR spectroscopy

Fig. 7 shows the FTIR spectra of representative ball milled BiVO_4 samples. Whatever the sample (as-prepared or annealed), an intense and broad band at 731 cm^{-1} with shoulders at 827 cm^{-1} can be observed. A weak and intense IR band at 470 cm^{-1} is also visible. According to the previous works, those IR bands correspond to the characteristic vibrations of monoclinic BiVO_4 [29–31]. The band at 731 cm^{-1} corresponds to absorptions of $\nu_1(\text{VO}_4)$ and that at 470 cm^{-1} is assigned to $\nu_3(\text{VO}_4)$ weak absorption of the Bi–O bond. The IR spectra present sharp and better resolved features with annealing. This is indicative of an improvement of the crystalline features as also testified by Raman and XRD measurements.

The general trend from these IR experiments is in agreement with the conclusions structural investigations. An increase of the time duration of milling and the post-synthesis annealing improve the crystalline structure and stabilize the monoclinic polytype of BiVO_4 .

4. Conclusion

Mechano-chemical synthesis method was used to obtain BiVO_4 nanoparticles with spherical-like morphology and average sizes about 20 nm. Different milling times and BPR parameter can modulate crystalline order and morphology of the nanopowders. Additionally, annealing treatments performed at suitable temperature, time and atmosphere contribute to stabilize the monoclinic phase of BiVO_4 . The relevant parameters for an optimized synthesis consist in minimal time duration as 6 h and BPR parameters as 10:1. The physical features were investigated by complementary methods, which characterize the structural and optical features of samples. Thus, XRD patterns confirmed the presence of monoclinic sheelite BiVO_4 crystal phase with respect to the treatment conditions. Particularly, sharp and well-resolved XRD lines indicate the good crystalline order involved in BiVO_4 nanoparticles with a net improvement after annealing. The vibrational properties probed by Raman and FT-IR spectrometries have confirmed also the major role of annealing leading to a monoclinic phase in agreement with the involved active modes from Raman and IR spectra. Finally the optical properties were found only slightly dependant on the synthesis conditions and annealing with a band gap in the range 2.4–2.3 eV. This amplitude of changes can be related to the good crystalline core of the nanoparticles and the resulting improvement by annealing may concerns mainly the outermost surface states. The applications of these nanoparticles directed toward the catalysis of water dissociation are under scope.

Acknowledgments

We acknowledge the financial support from European Union FP7-NMP EU-Mexico program under grant agreement no 263878/ by CONACYT no 125141. Prof. Miguel A. Garcia-Sanchez, Department of Organic Chemistry, UAM, Mexico D.F. is gratefully acknowledged for the help in UV–Visible diffuse reflectance measurements. Venkatesan Rajalingam is also thankful for the scholarship jointly provided by SEP and CINVESTAV. The authors are grateful to Dr. Marie-Pierre Crosnier-Lopez-LDOF-CNRS and University du Maine, for performing some XRD patterns and their fitting by Fullprof Software.

References

- [1] Y.D. Liu, H. Zheng, Z. Yuan, Y. Zhao, J. Wacławik, E.R. Ke, X. Zhu, J. Am. Chem. Soc. 131 (2009) 17885.
- [2] M. Li, L. Zhao, L. Guo, Int. J. Hydrogen Energy XXX (2010) 1.
- [3] Y. Hau Ng, A. Iwase, A. Kudo, R. Amal, J. Phys. Chem. Lett. 1 (2010) 2607.
- [4] P. Mei, M. Henderson, A. Kassiba, A. Gibaud, J. Phys. Chem. Solids 71 (2010) 1.
- [5] B. Pattier, M. Henderson, A. Poppl, A. Kassiba, A. Gibaud, J. Phys. Chem. B 114 (2010) 4424.
- [6] A. Kudo, K. Omori, H. Kato, J. Am. Chem. Soc. 121 (1999) 11459.
- [7] N.C. Castillo, A. Heel, T. Graule, C. Pulgarin, Appl. Catal. B 95 (2010) 335.

- [8] J. Yu, Y. Zhang, A. Kudo, J. Solid State Chem. 182 (2009) 223.
- [9] L. Li, B. Yan, J. Alloys Compd. 476 (2009) 624.
- [10] H. Jiang, H. Endo, H. Natori, M. Nagai, K. Kobayashi, J. Eur. Ceram. Soc. 28 (2008) 2955.
- [11] H.M. Zhang, J.B. Liu, H. Wang, W.X. Zhang, H. Yan, J. Nanopart. Res. 10 (2008) 767.
- [12] Y. Guo, X. Yang, M. Fengyan, K. Li, L. Xu, X. Yuan, Y. Guo, Appl. Surf. Sci. 256 (2010) 2215.
- [13] Y. Zhou, K. Vuille, A. Heel, B. Probst, R. Kontic, G.R. Patzke, Appl. Catal. A Gen. 375 (2010) 140.
- [14] W. Liu, L. Cao, G. Su, H. Liu, X. Wang, L. Zhang, Ultrason. Sonochem. 17 (2010) 669.
- [15] A. Galembeck, O.L. Alves, J. Mater. Sci. 37 (2002) 1923.
- [16] A.W. Sleight, H.Y. Chen, A. Ferretti, Mater. Res. Bull. 14 (1979) 1571.
- [17] T.S. Zhang, J. Ma, L.B. Kong, J. Mater. Res. 21 (2006) 71.
- [18] X. Lin, J. Xing, W. Wang, Z. Shan, F. Xu, F. Huang, J. Phys. Chem. C 111 (2007) 18288.
- [19] M.D. Segall, P.J.D. Lindan, M.J. Probert, C.J. Pickard, P.J. Hasnip, S.J. Clark, M.C. Payne, J. Phys. Condens. Matter 14 (11) (2002) 271.
- [20] B. Vidhya, S. Velumani, J.A. ArenasAlatorre, A. MoralesAcevedo, R. Asomoza, J.A. ChavezCarvayar, Mater. Sci. Eng. B 174 (2010) 216.
- [21] K. Shantha, G.N. Subbanna, K.B.R. Varma, J. Solid State Chem. 142 (1999) 41.
- [22] V.V. Zyryanov, Inorg. Mater. 41 (2005) 156.
- [23] J. Yu, A. Kudo, Chem. Lett. 34 (2005) 850.
- [24] M. Anpo, Y. Kubokawa, Rev. Chem. Intermed. 8 (1987) 105.
- [25] M. Anpo, H. Nakaya, S. Kodama, Y. Kubokawa, K. Domen, T. Onishi, J. Phys. Chem. 90 (1988) 1633.
- [26] D.H. Franklin, I.E. Wachs, J. Phys. Chem. 95 (1991) 5031.
- [27] R.L. Frost, D.A. Henry, M.L. Weier, W. Martens, J. Raman Spectrosc. 37 (7) (2006) 722.
- [28] A. Walsh, Y. .Yan, M.N. Huda, M.M. Al-Jassim, S. Wei, Chem. Mater. 21 (3) (2009) 547.
- [29] J.B. Liu, H. .Wang, S. .Wang, H. Yan, Mater. Sci. Eng. B 104 (2003) 36.
- [30] L. Zhang, D.R. Chen, X.L. Jiao, J. Phys. Chem. B 110 (2006) 2668.
- [31] M. Gotic, S. Music, M. Ivanda, M. Soufek, S. Popovic, J. Mol. Struct. 744 (2005) 535.